

## Research Article

Zhaonan Jin, Dan Lei, Yang Wang, Liangke Wu\*, and Ning Hu

# Influences of poling temperature and elongation ratio on PVDF-HFP piezoelectric films

<https://doi.org/10.1515/ntrev-2021-0070>

received August 9, 2021; accepted August 20, 2021

**Abstract:** Poly(vinylidene fluoride) (PVDF) and its copolymers exhibit excellent piezoelectric properties and are potential materials for high efficiency energy harvesting devices. In this study, poly(vinylidene fluoride-co-hexa-fluoropropylene) (PVDF-HFP) films are prepared by the solution casting method. The prepared film is then subjected to mechanical stretching and poling process. By adjusting the temperature of the poling process and the elongation ratio of the mechanical stretching process, the relative content of  $\beta$ -phase  $F(\beta)$  increases significantly, leading to high piezoelectric performance. The maximum output voltage of the PVDF-HFP films poled at 40°C reaches 3.67 V, 71% higher than that of the films poled at room temperature. Fourier transform infrared spectroscopy analysis (FTIR), XRD (X-ray diffraction), and differential scanning calorimetry are used to investigate the influences of mechanical stretching and poling process on the crystal structure to discover the enhancement mechanism. This work provides a straightforward and low-cost route to prepare high piezoelectric PVDF-HFP-based materials.

**Keywords:** PVDF-HFP, stretching, poling, piezoelectricity

## 1 Introduction

Energy harvesting is a technology that collects distributed energy around the environment and converts it into usable electricity [1]. Current energy collection devices

include solar energy collection devices, wind energy collection devices, vibration energy collection devices, etc. [2–4]. The power generation mechanisms are mainly static electricity, piezoelectric electricity, and electromagnetic electricity [4], among which the piezoelectric energy harvesting technology has the advantages of fast response, low cost, simple structure, no electromagnetic interference, convenient to handle, and so on ref. [5].

According to the material properties and composition, piezoelectric materials can be classified as single crystals, piezoelectric ceramics, piezoelectric polymers, and piezoelectric composites. Piezoelectric polymers mainly include poly(vinylidene fluoride) (PVDF) and its copolymers, polyvinylchloride and polypropylene [6], which possess the advantages of high chemical corrosion resistance, low mechanical impedance, and excellent flexibility [7], showing extraordinary promise for applications in energy harvesting [8]. PVDF and its copolymers possess the advantages of high piezoelectric coefficient, favorable biocompatibility, wide frequency response, promising flexibility, and easy processing. PVDF assesses at least five crystal phases, i.e.,  $\alpha$ ,  $\beta$ ,  $\delta$ ,  $\gamma$ , and  $\varepsilon$ . The  $\alpha$ -phase is monoclinic and the chain configuration is TGTG'. The  $\beta$ -phase belongs to the orthomorphous system and the molecular chain configuration is TTT. The  $\gamma$ -phase is monoclinic and its chain structure is similar to that of the  $\alpha$ -crystal phase [7]. Among the phases, the  $\alpha$ -crystal phase is nonpolar, so it does not exhibit piezoelectricity. The  $\beta$ -crystal phase is the most strongly polar with excellent piezoelectricity [9]. In most cases, the  $\alpha$ -phase dominates in the crystal parts of PVDF. Therefore, increasing the  $\beta$ -phase content plays an extremely important role in the improvement of PVDF's piezoelectricity. At present, uniaxial stretching [10–12], high electric field poling [13–15], high pressure crystallization [16,17], and nanofillers additions [12,18,19] are commonly applied to increase the content of the  $\beta$ -crystal phase.

The influences of poling temperature on piezoelectric properties of materials have been studied in a multitude of reports [21–24]. The poling effects on the piezoelectric properties of 0–3 connectivity PZT Portland cement (PC) composites, including piezoelectric coefficient ( $d_{33}$ ) and electromechanical coupling factor ( $k_T$ ), have been

\* Corresponding author: Liangke Wu, College of Aerospace Engineering, Chongqing University, Chongqing 400044, China, e-mail: wuliangke@cqu.edu.cn, tel: +86-02365102510

Zhaonan Jin, Dan Lei, Yang Wang: College of Aerospace Engineering, Chongqing University, Chongqing 400044, China

Ning Hu: College of Aerospace Engineering, Chongqing University, Chongqing 400044, China; School of Mechanical Engineering, Hebei University of Technology, Tianjin 300401, China

investigated by Jaitanong and Chaipanich. The results demonstrate that when the poling temperature is set at 130°C, the  $d_{33}$  and  $k_t$  reach the maximum values [20]. Some researchers also proposed that the piezoelectric ceramics with polycrystalline phase boundary are affected by poling temperature, and the piezoelectric constants are highly sensitive to the poling temperature [21–24].

As mentioned above, most of the published studies about the effects of poling temperature on the piezoelectric properties are focused on piezoelectric ceramics, with only a few on PVDF or other polymers. It was reported that under the poling electric field of 150 MV m<sup>-1</sup> at 95°C, the nonpolar  $\alpha$ -crystal phase can be transformed to the polar  $\beta$ -crystal phase [25]. Darestani *et al.* investigated the piezoelectric properties of piezoelectric PVDF films for separation processes. The specimen was heated from room temperature to 90 ± 10°C, while the poling electric field increased gradually from zero to 2 kV at a rate of ~50 V min<sup>-1</sup>. The results show that the poling process dramatically changes the microstructure of the films [26]. Most studies emphasized that the structural evolution may be due to the internal rotation of the molecular chains induced by the electric field. It is in consistent with the  $\beta$ -phase formation and the rearrangement of the inherent dipoles in the matrix. In these studies, the effect of the poling on the structure of PVDF is mentioned only when the heating is also carried out during poling [25–27]. Besides, Jan proposed that the relative content of the  $\beta$ -crystal phase increases significantly when the poling temperature is set at 150°C [28]. As a conclusion, both the temperature and the poling electric field may have effects on the piezoelectric properties of the materials by affecting phase evolution and realignment of dipole moments. The content and orientation polarizability of the  $\beta$ -crystal phase are improved when poled at a proper temperature as shown in the experiments. After the optimal poling temperature was obtained, we also varied the elongation ratio during the stretching process to define the optimal preparation parameters.

## 2 Experiments

### 2.1 Materials

PVDF can form a number of different copolymers. Poly(vinylidene fluoride-co-hexafluoropropylene) (PVDF-HFP) is a PVDF copolymer of low crystallinity, but high F content compared with PVDF; consequently, it exhibits better

**Table 1:** The properties of PVDF-HFP

|                  |              |  |                             |
|------------------|--------------|--|-----------------------------|
| Morphology       | White powder | Density                                      | 1.76–1.8 g cm <sup>-3</sup> |
| Melting point    | 140–145°C    | Water absorption                             | 0.03%                       |
| Refractive index | 1.41         | Melt viscosity (232°C, 100 s <sup>-1</sup> ) | 2,300–2,700 Pa s            |

hydrophobicity than PVDF. Besides, PVDF-HFP also exhibits better flexibility and solidification. In terms of piezoelectric properties, when the mixing ratio of HFP is 5%, the piezoelectric coefficient  $d_{31}$  of PVDF-HFP can reach 30 p CN<sup>-1</sup>, which is higher than that of PVDF [29].

The PVDF-HFP powder (Kynar Flex 2801) is produced by Arkema Inc. Its properties are shown in Table 1. The solvent is *N,N*-dimethylformamide (DMF) which can be commercially obtained from Shanghai Titan Scientific Co., Ltd.

### 2.2 Preparation of piezoelectric films

In this study, the solution casting method is used to prepare the initial crystallized films. The preparation process of the initial crystallization films mainly includes the following steps as shown in Figure 1: (1) add moderate PVDF-HFP powder into DMF solution (mass ratio: PVDF-HFP:DMF = 1:3) by a planetary machine for 5 min and an ultrasonic machine for 5 min, then by a planetary machine for 5 and 2 min (for defoaming). (2) Pour the DMF/PVDF-HFP mixture evenly onto a 2 mm-thick Al mold whose edges are formed by sponge tapes (9 cm × 16.5 cm) which are removed within 10 min after solution casting, and heat it at 90°C for 2 h; (3) Cut the samples for stretching from the middle of the initial crystallization films, the size is 5.5 cm × 4 cm (stretching direction). The thickness of the initial crystallized films ranges from 180 to 240  $\mu$ m. (4) Press the initial crystallized film by a heavy flat mass for 24 h. (5) Stretch the films at about 60°C in a temperature-control box (±2°C) with a rate of 10 mm min<sup>-1</sup> and an elongation ratio  $R$  of 4.5–5.5 [14]. The film stretching equipment is shown in Figure 1(c), which includes an EZ-LX tensile testing machine (Shimadzu Manufacturing Co. Ltd., Japan), a homemade temperature-control box, a digital heat gun, a digital thermometer, *etc.* The thickness of the stretched films is 50 to 90  $\mu$ m, as shown in Figure 2. (6) Attach Al electrodes ( $t = 15 \mu$ m) on both sides of the film by CW2400 conductive epoxy adhesive and keep it for 24 h for complete curing. The poling process was

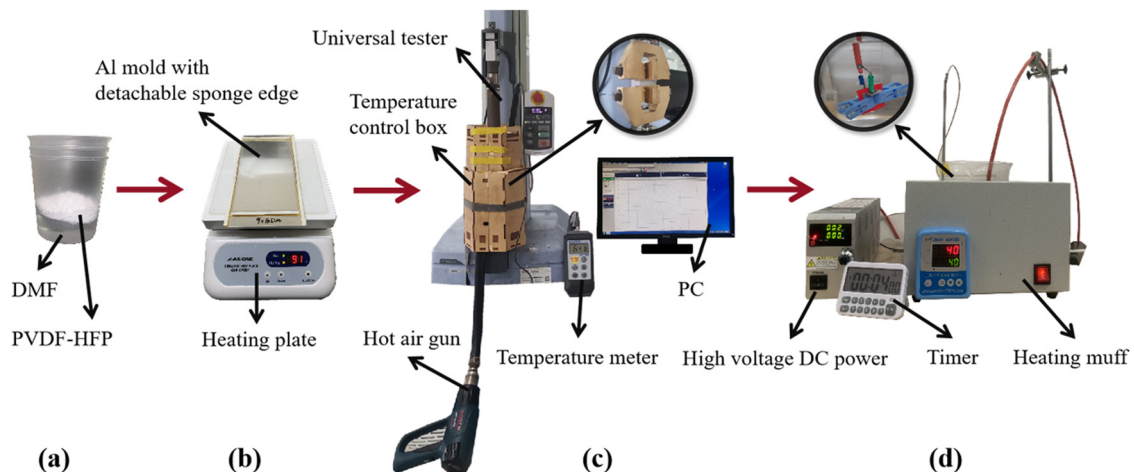


**Figure 1:** Preparation process of PVDF-HFP piezoelectric films: (a) solution, (b) initial crystallization, (c) uniaxial stretching, and (d) stepwise poling.

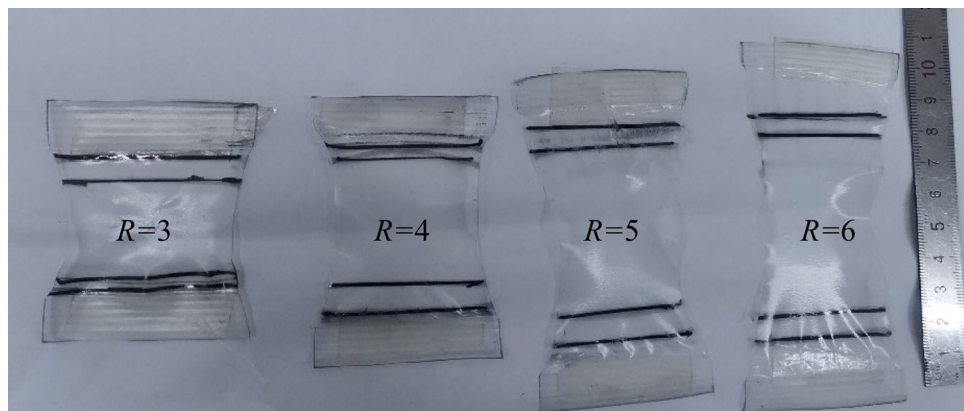


**Figure 2:** Images of stretched films with different elongation ratios.

carried out in silicone oil at various temperatures by a stepwise method. The voltage source is HJPQ-30P1 (Matsumada Precision Inc.). The initial electric field is  $20 \text{ MV m}^{-1}$ , and the maximum electric field (denoted as  $E_{\max}$ ) is  $90 \text{ MV m}^{-1}$ . For each step, the poling time is 8 min, the rest time is 4 min, and the electric field increases by  $10 \text{ MV m}^{-1}$ .

To study the effects of poling temperature on the piezoelectric properties of PVDF-HFP, the poling temperature (denoted as  $T_p$ ) is set from 25 to  $45^\circ\text{C}$ , and the elongation ratio in the stretching process is kept at 5. Figure 1(d) shows the equipment for poling. The poling is carried out in silicone oil heated by a digital electric heating sleeve ( $\pm 2^\circ\text{C}$ ). After the optimal poling temperature is determined, the elongation ratio varies from 3 to 6 to investigate its effects on piezoelectricity.

The measurement setup of the open circuit voltage is shown in Figure 3. The measurement method is introduced in a previous report [12] and in the Supporting information's Section at the end of the paper.

## 2.3 Characterization of piezoelectric films

FTIR spectra were used to identify the structure of the polymer backbone, the types and positions of substituents, and the structure of the molecular chains. The equipment used in this study was the Nicolet IS50 Fourier Transform Infrared Spectrometer (Thermo Fisher Scientific Co. Ltd., USA).

X-ray diffraction (XRD) is a technique for structural analysis of crystalline substances. In the characterization

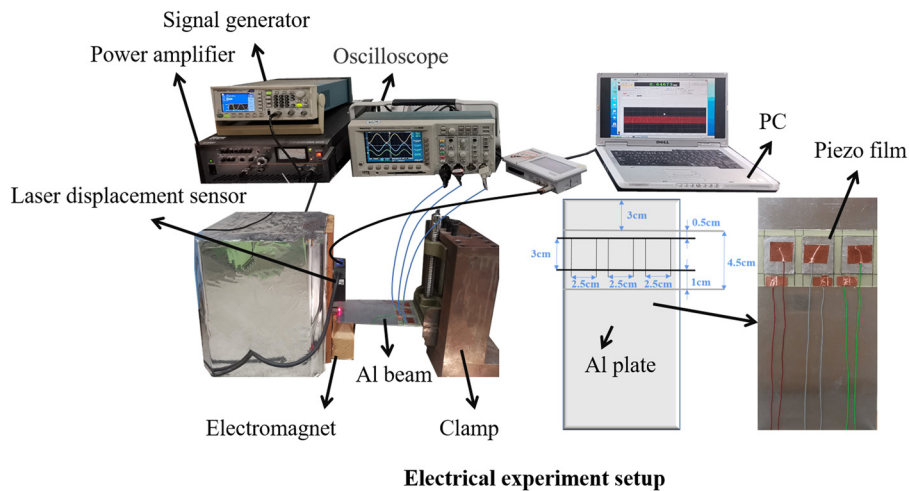


Figure 3: Measurement setup of the open circuit voltage.

of polymers, XRD is mainly used for phase analysis and crystallinity degree determination. In this study, the equipment used for XRD was X'PERT POWDER X-ray diffractometer (Panaco Co. Ltd., Netherlands).

Differential scanning calorimetry (DSC) is a thermal analysis technique that measures the relationship between temperature and the power difference input into the sample and reference material. It can be used to study the thermal change in the reaction process such as melting, sublimation, and crystallization. The Netzsch DSC 214 Polyma differential scanning calorimeter was used in this study.

### 3 Results and discussion

#### 3.1 Open circuit voltage

It was proved that the open circuit voltage  $V$  is proportional to the film thickness ( $t$ ) and the displacement ( $u$ ) of the end of the vibration cantilever [19]. Therefore, the concept of calibrated open circuit voltage ( $V_c$ ) is introduced in this study to evaluate the piezoelectric properties of different piezoelectric films. The calculation formula of  $V_c$  is:

$$V_c = V \frac{u_0 t_0}{u t}, \quad (1)$$

where  $V$  is the actual measured voltage,  $u$  is the displacement of the end of the aluminum plate,  $t$  is the film thickness,  $u_0 = 1.0 \text{ mm}$  is the standard displacement, and  $t_0 = 100.0 \mu\text{m}$  is the standard thickness.

Figure 4(a) shows the relationship between the calibrated open circuit voltage and the poling temperature  $T_p$  when the elongation ratio is kept at 5. It is shown that the open circuit voltage increases with the poling temperature. However, an excessively high temperature may lead to the electric breakdown at a relatively lower electric field. Figure 4(b) shows the relationship between the calibrated open circuit voltage and the elongation ratio  $R$  when the poling temperature is kept at 40°C. From the experimental results, it is observed that the open circuit voltage of PVDF-HFP films increases with poling temperature until 40°C. However, when the poling temperature rises to 45°C, electrical breakdown [30] occurs when the poling electric field intensity is higher than  $60 \text{ MV m}^{-1}$ . As a result, when the poling temperature is set to 45°C, the maximum electric field of poling is  $60 \text{ MV m}^{-1}$  (For other samples,  $E_{\max} = 90 \text{ MV m}^{-1}$ ). When  $T_p$  is 40°C and  $R$  is 5, the calibrated open circuit voltage reaches the highest value of 3.67 V, which is 71% higher than that of the films poled at room temperature (2.15 V) (Figure 4(a)). When  $T_p$  is 45°C and the maximum poling electric field  $E_{\max}$  is  $60 \text{ MV m}^{-1}$ , the calibrated open circuit voltage is only 2.05 V. Thus, the optimal poling temperature in this study is determined to be 40°C.

At the optimal poling temperature of 40°C, the open circuit voltages of films stretched by different elongation ratios (3–6) were also measured. The experimental results showed that the open circuit voltage increases with  $R$  until 5 ( $V_c = 3.67 \text{ V}$ ) and then decreases (Figure 4(b)). It is found that the open circuit voltage increases with the elongation ratio and reaches the maximum value at  $R = 5$  and then decreases. The phase transformation mainly occurs when  $R < 4$ , thus  $F(\beta)$  remains nearly unchanged when  $R > 4$ .

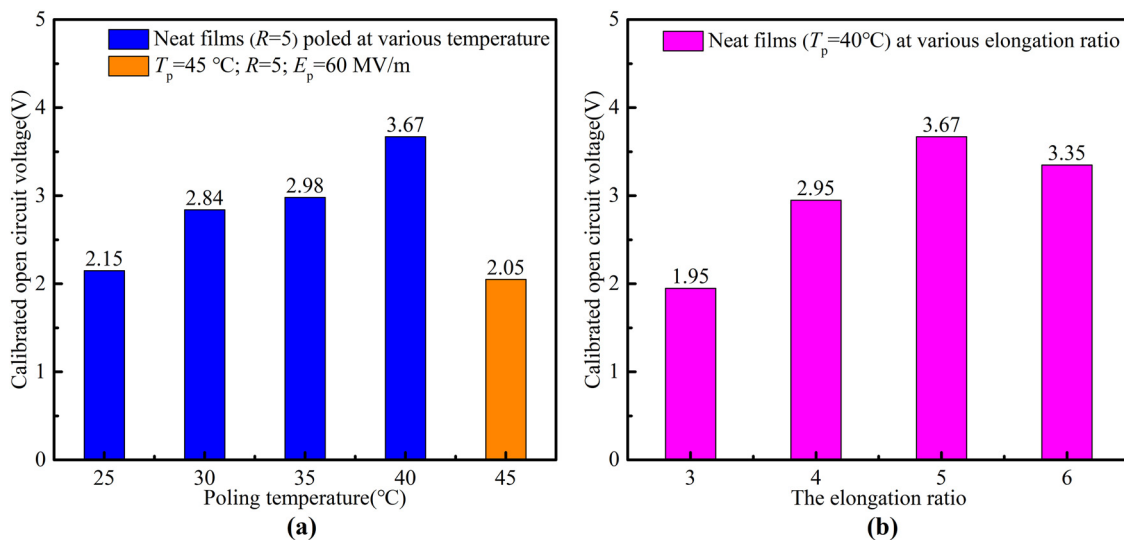


**Figure 4:** The calibrated open circuit output voltages of PVDF-HFP films: (a) PVDF-HFP films ( $R = 5$ ) poled at various temperatures; (b) PVDF-HFP films ( $T_p = 40^\circ\text{C}$ ) stretched at various elongation ratios.

However, the alignment of molecular chains along the stretching direction continues when the elongation ratio increases from 4 to 5, which leads to better piezoelectricity. But more crystalline defects are formed when the elongation ratio increases further, which results in the reduction of piezoelectricity. The experimental results indicate that  $R = 5$  and  $T_p = 40^\circ\text{C}$  are the optimal parameters to produce high piezoelectric PVDF-HFP films.

### 3.2 FTIR

For PVDF-HFP films, FTIR is usually used to investigate the crystal structure. The  $\alpha$ -crystal phase is the most common crystal phase in the initial crystallized films (non-stretched) with characteristic peaks of 489, 614, 766, 795, 855, and  $976\text{ cm}^{-1}$  [31]. The characteristic peaks of the  $\beta$ -phase are at 510, 840, and  $1,279\text{ cm}^{-1}$  [32]. The relative fraction of the  $\beta$ -phase  $F(\beta)$  is an extremely important parameter in the preparation of PVDF piezoelectric films, which can be calculated by equation (2):

$$F(\beta) = \frac{A_\beta}{\left(\frac{K_\beta}{K_\alpha}\right)A_\alpha + A_\beta} = \frac{A_\beta}{1.26A_\alpha + A_\beta}, \quad (2)$$

where  $K_\alpha$  is  $6.1 \times 10^4\text{ cm}^2\text{ mol}^{-1}$ ,  $K_\beta$  is  $7.7 \times 10^4\text{ cm}^2\text{ mol}^{-1}$ , and  $A_\alpha$  and  $A_\beta$  are the areas of the absorption peaks near  $766$  and  $840\text{ cm}^{-1}$ , respectively [7]. In this work, the integrating range is the peak ( $766\text{ cm}^{-1}$  for  $A_\alpha$  and  $840\text{ cm}^{-1}$   $A_\beta$ )  $\pm 10\text{ cm}^{-1}$ . For simplicity, the stretched films are

**Table 2:** Relative fraction of  $\beta$ -phase  $F(\beta)$  of PVDF-HFP films poled at various temperatures ( $R = 5$ )

| $T_p$ ( $^\circ\text{C}$ ) | 25 | 30 | 35 | 40 | 45 ( $E_p = 60\text{ MV m}^{-1}$ ) |
|----------------------------|----|----|----|----|------------------------------------|
| $F(\beta)$ (%)             | 87 | 96 | 96 | 97 | 92                                 |

**Table 3:** Relative fraction of  $\beta$ -phase  $F(\beta)$  of PVDF-HFP films stretched at various elongation ratios ( $T_p = 40^\circ\text{C}$ )

| $R$     | 3  | 4  | 5  | 6  |
|---------|----|----|----|----|
| $S$ (%) | 61 | 74 | 80 | 76 |
| SP (%)  | 68 | 93 | 97 | 96 |

$F(\beta)$  of untreated films ( $R = 1$ ) is 14%.

denoted by  $S$ , and the stretched and poled films are denoted as  $SP$ .

As shown in Tables 2 and 3 and Figure 5, when the elongation ratio  $R$  is 5 and the maximum poling electric field  $E_{\max}$  is  $90\text{ MV m}^{-1}$ , almost only  $\beta$ -phase exists when the poling temperature is over  $30^\circ\text{C}$ . The  $F(\beta)$  of samples poled at  $45^\circ\text{C}$  and  $60\text{ MV m}^{-1}$  is slightly lower than other samples. During the poling process, the electric field forces the dipole moments to align along the electric field direction, and thus the piezoelectricity is improved. Besides, for the samples of lower  $F(\beta)$ , the induced stress by the electric field also promotes the  $\alpha$ - to  $\beta$ -phase transformation to some extent. In Figure 5, the sample O (sample:  $R = 5$ ,  $T_p = 45^\circ\text{C}$ ) contains a substantial  $\alpha$ -phase. It is attributed to the transformation from  $\gamma$  to  $\alpha$  phase at a

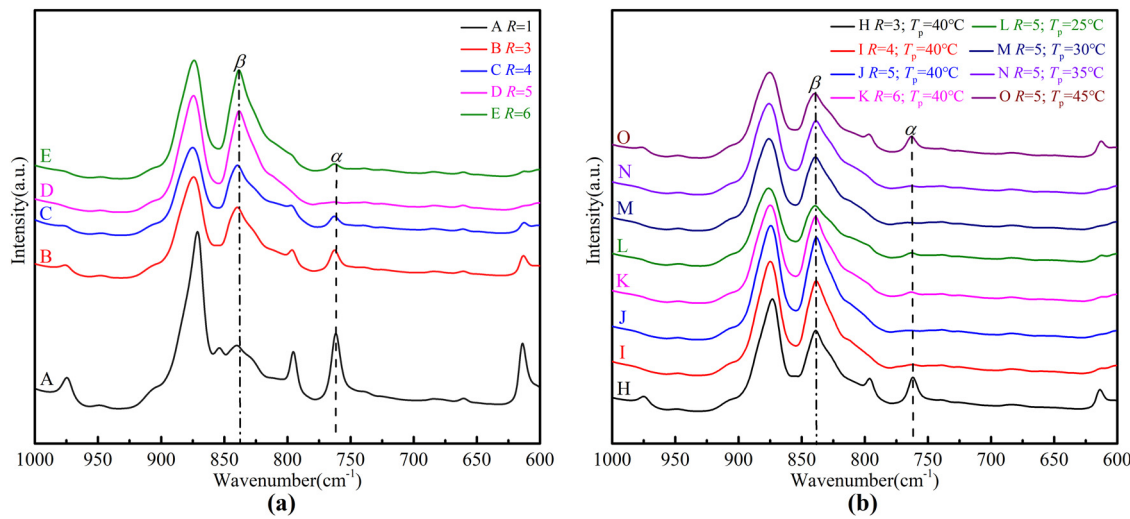


**Figure 5:** FTIR spectra of PVDF-HFP films: (a) stretched PVDF-HFP films at various elongation ratios. (b) Stretched and poled PVDF-HFP films at various elongation ratios ( $T_p = 40^\circ\text{C}$ ) or various poling temperatures ( $R = 5$ ).

relative higher temperature. The relative lower electric field cannot increase the  $\beta$ -phase formation effectively [33]. When  $T_p$  is  $40^\circ\text{C}$ ,  $R$  is 5, and  $E_{\text{max}}$  is  $90 \text{ MV m}^{-1}$ , the samples generate the highest open circuit voltages

as shown in Figure 4, indicating the complete realignment of dipole moments compared to other samples.

### 3.3 XRD

XRD was carried out by  $\text{CuK}\alpha$  radiation with  $2\theta$  from  $10^\circ$  to  $30^\circ$  and the scan rate of  $1^\circ \text{ min}^{-1}$ . The characteristic peaks of the  $\alpha$ - and  $\beta$ -crystal phases in PVDF and their copolymers are shown in Table 4. It should be noted that little shifts of characteristic peaks may exist in different experiments. As shown in Figure 6, the characteristic

**Table 4:** Characteristic angles of  $\alpha$ -phase and  $\beta$ -phase in PVDF and its copolymers [38–40]

| Crystal phase | Characteristic angles (plane)   |
|---------------|---|
| $\alpha$      | $17.8^\circ(020)$ , $18.4^\circ(100)$ , $20.0^\circ(110)$ , $26.6^\circ(021)$ |
| $\beta$       | $20.4^\circ(110,200)$ , $36.3^\circ$  |

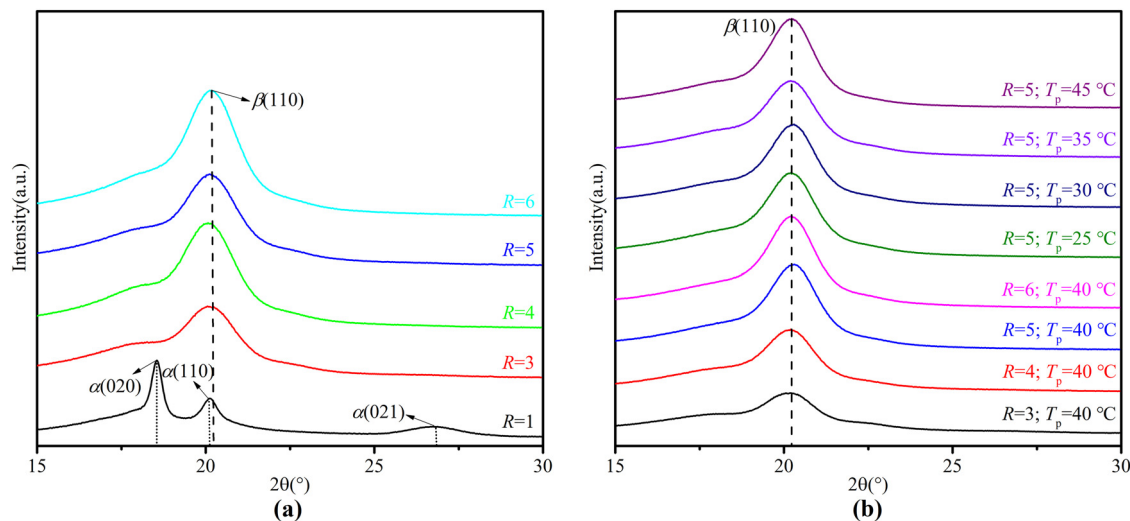


**Figure 6:** XRD diffraction spectrogram of PVDF-HFP films: (a) stretched plus poled films at various elongation ratios ( $T_p = 40^\circ\text{C}$ ) and various poling temperatures ( $R = 5$ ); (b) stretched films at various elongation ratios.

**Table 5:** Crystallinity degree  $X_c$  of PVDF-HFP films poled at various temperatures ( $R = 5$ )

| $T_p$ (°C) | 25 | 30 | 35 | 40 | 45 ( $E_p = 60$ MV m $^{-1}$ ) |
|------------|----|----|----|----|--------------------------------|
| $X_c$ (%)  | 37 | 40 | 37 | 41 | 40                             |

**Table 6:** Crystallinity degree of  $X_c$  of PVDF-HFP stretched films at various elongation ratios ( $T_p = 40$  °C)

| $R$    | 3  | 4  | 5  | 6  |
|--------|----|----|----|----|
| S (%)  | 35 | 37 | 39 | 40 |
| SP (%) | 36 | 39 | 41 | 41 |

$X_c$  of untreated films ( $R = 1$ ) is 28%.

peaks of both  $\alpha$ -phase and  $\beta$ -phase exist in the non-stretched samples. However, in the stretched samples, the characteristic peaks of the  $\alpha$ -phase nearly disappear. Compared with the stretched films and poled samples, the spectra seem no obvious differences. Therefore, the  $\alpha$ - to  $\beta$ -phase transformation mainly occurs in the stretching process. In the poling process, it is not so obvious since  $F(\beta)$  is quite high in the stretched films. The main effect of poling is the realignment of the dipole moments in the PVDF-HFP matrix, and thus piezoelectricity can be obtained.

According to the experimental results, the characteristic peaks appear at 18.5°, 20.1°, and 26.7° in the films before stretching, which correspond to the plane of the  $\alpha$ -phase, but the characteristic peaks of the  $\beta$ -phase are not obvious. It can be seen that the  $\beta$ -phase is dominant in

the samples after stretching and heated-poling (Figure 6(b)). Combining with the FTIR results, it can be concluded that the stretching is the main factor for high  $\beta$ -phase, and poling can promote the  $\alpha$ - to  $\beta$ -phase transformation in the samples of low  $F(\beta)$ . However, for high  $\beta$ -phase samples, it does little.

### 3.4 DSC

In the DSC process, the samples were cut into pieces of 3 mm $^2$  × 3 mm $^2$ . The sample was first preserved at 40°C for 5 min and then heated from 40 to 200°C at a rate of 10°C min $^{-1}$ . The following equation was used to calculate the crystallinity degree ( $X_c$ ) of PVDF-HFP films [33]:

$$X_c = \left( \frac{\Delta H_m}{\Delta H_m^\phi} \right) \times 100\%, \quad (3)$$

where  $\Delta H_m$  is the melting enthalpy of the material which can be calculated by the DSC software, and  $\Delta H_m^\phi$  is the melting enthalpy of 100% crystalline PVDF-HFP, *i.e.*, 104.5 J g $^{-1}$  [34].

The crystallinity degree of PVDF-HFP films is shown in Tables 5 and 6, and the DSC spectra are shown in Figure 7. It is observed that the crystallinity degree of the PVDF-HFP films increases after stretching, indicating that the concentration stress applied on the amorphous area can force the molecular chains to form crystal structure, which is consistent with the published data by Cai *et al.* [35]. While the  $X_c$  decrement was also reported [14],

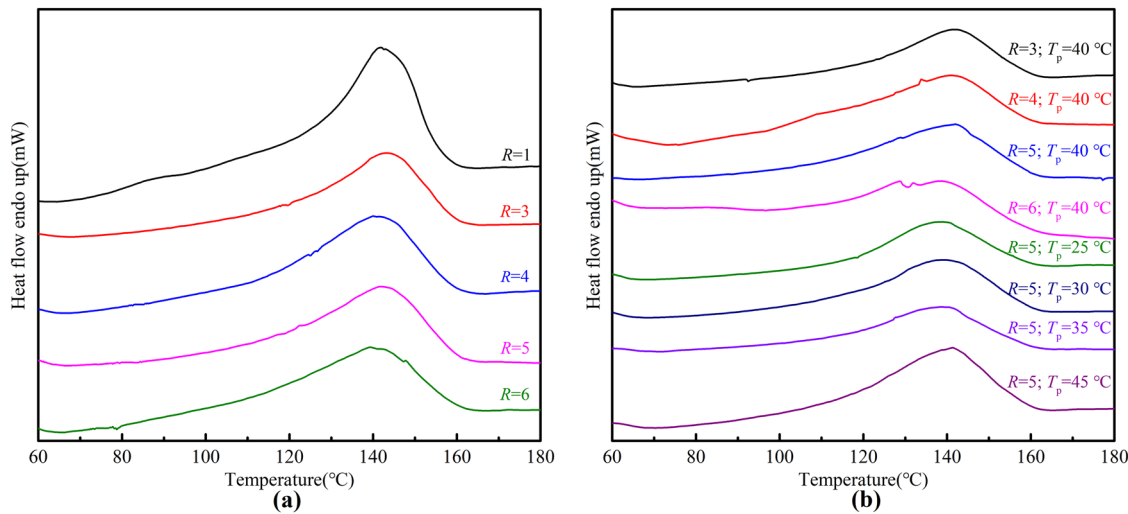


**Figure 7:** DSC thermograms of PVDF-HFP films: (a) stretched PVDF-HFP films at various elongation ratios; (b) stretched plus poled PVDF-HFP films at various elongation ratios ( $T_p = 40$  °C) and various poling temperatures ( $R = 5$ ).

for higher draw ratios the polymer chains become more oriented, which results in the phase transformation accompanied by a decrease of the crystallinity degree. It reflects that the influence of stretching on crystallinity is complicated. In this work, the increase of  $X_c$  is attributed to the stress work on the amorphous area which forces part of the molecular chains to align in the  $\beta$ -phase. On the other hand, crystallization defects may arise during the stretching process [36,37]. From Table 6, the crystallinity degree changes little after poling, indicating it works little on the crystallinity degree, because it cannot provide enough stress on the molecular chains in the amorphous region to form crystal structure [28]. The main effect of poling is the realignment of dipole moments, as reflected by the change of the open circuit voltage.

## 4 Conclusion

In this study, the influences of poling temperature and elongation ratios on phase transformation and output voltages of PVDF-HFP films are investigated. The FTIR and XRD spectra demonstrate that the  $\alpha$ - to  $\beta$ -phase mainly occurs in the stretching process ( $R \geq 3$ ) due to molecular chain elongation caused by the external force. The poling temperature has strong effects on the piezoelectricity of PVDF-HFP films. It is found that the output open circuit voltage increases with the temperature until 40°C. While the temperature is 45°C, the poling fails when the electric field is over 60 MV m<sup>-1</sup>. Thus, the piezoelectricity cannot be further increased. The optimal parameters are defined as  $R = 5$ ,  $T_p = 40^\circ\text{C}$ , and  $E_{\text{max}} = 90 \text{ MV m}^{-1}$ . At this condition, the open circuit voltage reaches 3.67 V, 71% higher than that of samples poled at 25°C. The experimental method of heated-poling reported in this study is facile and of low cost for preparing efficient piezoelectric films.

**Funding information:** This work was financially supported by National Natural Science Foundation of China (No. 51703015) and Fundamental Research Funds for the Central Universities (No. 2020CDJQY-A008).

**Author contributions:** All authors have accepted responsibility for the entire content of this manuscript and approved its submission.

**Conflict of interest:** The authors state no conflict of interest.

**Data availability statement:** The authors confirm that the data supporting the findings of this study are available within the article and its supplementary materials.

## References

- Wan CY, Bowen CR. Multiscale-structuring of polyvinylidene fluoride for energy harvesting: the impact of molecular-, micro- and macro-structure. *J Mater Chem A*. 2017;5(7):3091–128.
- Schonecker A, Laas L, Gutjahr A, Wyers P, Reinink A, Wiersma B. Ribbon-growth-on-substrate: Progress in high-speed crystalline silicon wafer manufacturing. *Photovoltaic Specialists Conference (PVSC)*. New Orleans, LA, USA: IEEE; 2002 May 19–24.
- Abdelkefi A. Aeroelastic energy harvesting: a review. *Int J Eng Sci*. 2016;100:112–35.
- Kodali P, Mahidhar MN, Lokesh N, Prasad MVN, Sambandan S. Vibration energy harvesting. *2012 International Conference on Emerging Electronics (ICEE)*. Mumbai, India: IEEE; 2012 Dec 15–17.
- Erturk A, Inman DJ. *Piezoelectric energy harvesting*. West Sussex: John Wiley & Sons; 2011.
- Gai XZ. Direction of research and development and status for piezoelectric. *China Ceram*. 2008;44(5):9–13.
- Martins P, Lopes AC, Lanceros-Méndez S. Electroactive phases of poly(vinylidene fluoride): determination, processing and applications. *Prog Polym Sci*. 2014;39(4):683–706.
- Karen SK, Mandal D, Khatua BB. Self-powered flexible Fe-doped RGO/PVDF nanocomposite: an excellent material for a piezoelectric energy harvester. *Nanoscale*. 2015;7(24):10655–66.
- Kim GH, Hong SM, Seo Y. Piezoelectric properties of poly(vinylidene fluoride) and carbon nanotube blends:  $\beta$ -phase development. *Phys Chem Chem Phys*. 2009;11(44):10506–12.
- Salimi A, Yousefi AA. Analysis method: FTIR studies of  $\beta$ -phase crystal formation in stretched PVDF films. *Polym Test*. 2003;22(6):699–704.
- Gomes J, Serrado Nunes J, Sencadas V, Lanceros-Mendez S. Influence of the  $\beta$ -phase content and degree of crystallinity on the piezo- and ferroelectric properties of poly(vinylidene fluoride). *Smart Mater Struct*. 2010;19(6):065010.
- Wu L, Yuan W, Hu N, Wang Z, Chen C, Qiu J, et al. Improved piezoelectricity of PVDF-HFP/carbon black composite films. *J Phys D Appl Phys*. 2014;47(13):13502.
- Dadi S, Paul R, Michael W. The step-wise poling of VDF/TrFE copolymers. *Ferroelectrics*. 1996;186:255–8.
- Sencadas V, Gregorio R, Lanceros-Méndez S.  $\alpha$  to  $\beta$ -phase transformation and microstructural changes of PVDF films induced by uniaxial stretch. *J Macromol Sci Phys*. 2009;48(3):514–25.
- Ting Y, Gunawan H, Sugono A, Chiu CW. A new approach of polyvinylidene fluoride (PVDF) poling method for higher electric response. *Ferroelectrics*. 2013;446(1):28–38.
- Scheinbeim JI, Nakafuku C, Newman BA, Pae KD. High-pressure crystallization of poly(vinylidene fluoride). *J Appl Phys*. 1979;50(6):4399–405.

[17] Hattori T, Kanaoka M, Ohigashi H. Improved piezoelectricity in thick lamellar  $\beta$ -form crystals of poly(vinylidene fluoride) crystallized under high pressure. *J Appl Phys.* 1996;79(4):2016–22.

[18] Satish B, Sridevi K, Vijaya MS. Study of piezoelectric and dielectric properties of ferroelectric PZT-polymer composites prepared by hot-press technique. *J Phys D Appl Phys.* 2002;35(16):2048–50.

[19] Shanks L, Siddiqui MR, Kliescikova J, Pearce N, Ariti C, Muluneh L, et al. High-performance flexible lead-free nanocomposite piezoelectric nanogenerator for biomechanical energy harvesting and storage. *Nano Energy.* 2015;15:177–85.

[20] Jaitanong N, Chaipanich A. Effect of poling temperature on piezoelectric properties of 0–3 PZT-Portland cement composites. *Ferroelectr Lett.* 2008;35(1–2):17–23.

[21] Huan Y, Wang X, Zhang S, Gao R, Li L. Effect of poling temperature on piezoelectric coefficient in  $(Na_{0.52}K_{0.4425}Li_{0.0375})(Nb_{0.86}Ta_{0.06}Sb_{0.08})O_3$  ceramics. *Phys Status Solidi A.* 2013;210(12):2579–82.

[22] Du HL, Zhou WC, Luo F, Zhu DM. An approach to further improve piezoelectric properties of  $K_{0.5}Na_{0.5}NbO_3$ -based lead-free ceramics. *Appl Phys Lett.* 2007;91(20):202907.

[23] Li BZ, Blendell JE, Bowman KJ. Temperature-dependent poling behavior of lead-free BZT–BCT Piezoelectrics. *J Am Ceram Soc.* 2011;94(10):3192–4.

[24] Wu J, Xiao D, Wu W, Chen Q, Zhu J, Yang Z, et al. Composition and poling condition-induced electrical behavior of  $(Ba_{0.85}Ca_{0.15})(Ti_{1-x}Zr_x)O_3$  lead-free piezoelectric ceramics. *J Eur Ceram Soc.* 2012;32(4):891–8.

[25] Ye Y, Jiang Y, Wu ZM, Zeng HJ. Phase transitions of poly(vinylidene fluoride) under electric fields. *Integr Ferroelectr.* 2006;80(1):245–51.

[26] Darestani MT, Coster HGL, Chilcott TC, Fleming S, Nagarajan V, An H. Piezoelectric membranes for separation processes: fabrication and piezoelectric properties. *J Membr Sci.* 2013;434:184–92.

[27] Darestani MT, Chilcott TC, Coster HGL. Effect of poling time on filtration properties of PVDF membranes treated in intense electric fields. *Polym Bull.* 2014;71(4):951–64.

[28] Kulek J, Hilczer B, Szlaferk A. Effect of the poling temperature on the dielectric properties of oriented PVDF film. *Ferroelectrics.* 1988;81:1329–32.

[29] Zhang LL, Guo SS. Progress in the ferroelectric poly(vinylidene fluoride) and its copolymers. *Prog Phys.* 2016;36(2):35–45.

[30] Zhu XH. Effects of cross-linking method on insulation properties of cross-linked polyethylene [PhD dissertation]. Tientsin University; 2010.

[31] Boccaccio T, Bottino A, Capannelli G, Piaggio P. Characterization of PVDF membranes by vibrational spectroscopy. *J Membr Sci.* 2002;210(2):315–29.

[32] Li L, Zhang MQ, Rong MZ, Ruan WH. Studies on the transformation process of PVDF from  $\alpha$  to  $\beta$  phase by stretching. *RSC Adv.* 2014;4(8):3938–43.

[33] Pramanick A, Misture S, Osti NC, Jalarvo N, Diallo SO, Mamontov E. Ferroelectric to paraelectric phase transition mechanism in poled PVDF-TrFE copolymer films. *Phys Rev B Condens Matter.* 2017;96(17):174103.

[34] Lanceros-Méndez S, Mano JF, Costa AM, Schmidt VH. FTIR and DSC studies of mechanically deformed  $\beta$ -PVDF films. *J Macromol Sci Phys.* 2001;B40(3–4):517–27.

[35] Cai J, Hu N, Wu L, Liu Y, Li Y, Ning H, et al. Preparing carbon black/graphene/PVDF-HFP hybrid composite films of high piezoelectricity for energy harvesting technology. *Compos Part A Appl Sci Manufac.* 2019;121:223–31.

[36] Cui Z, Hassankiadeh NT, Zhuang Y, Drioli E, Lee YM. Crystalline polymorphism in poly(vinylidene fluoride) membranes. *Prog Polym Sci.* 2015;51:94–126.

[37] Ye H, Xu C, Meng N, Meng Z, Xu L. High energy density and charge-discharge efficiency of uniaxial stretched poly(vinylidene fluoride-hexafluoropropylene) film with electroactive phase conversion. *J Mater Sci Mater Electron.* 2018;29(8):6619–31.

[38] Mohammadi B, Yousefi AA, Bellah SM. Effect of tensile strain rate and elongation on crystalline structure and piezoelectric properties of PVDF thin films. *Polym Test.* 2007;26(1):42–50.

[39] Gregorio JrR, Nociti NCPD. Effect of PMMA addition on the solution crystallization of the alpha and beta phases of poly(vinylidene fluoride) (PVDF). *J Phys D Appl Phys.* 1995;28(2):432–6.

[40] Gregorio JrR, Capitão RC. Morphology and phase transition of high melt temperature crystallized poly(vinylidene fluoride). *J Mater Sci.* 2000;35(2):299–306.